Single-Neutron States in ^{101}Sn

D. Seweryniak,[1] M. P. Carpenter,[1] S. Gros,[1] A. A. Hecht,[2] N. Hoteling,[2] R. V. F. Janssens,[1] T. L. Khoo,[1] T. Lauritsen,[1]
C. J. Lister,[1] G. Lotay,[3] D. Peterson,[1] A. P. Robinson,[1] W. B. Walters,[2] X. Wang,[4] P. J. Woods,[3] and S. Zhu[1]

[1]*Argonne National Laboratory, Argonne, Illinois, 60439, USA*
[2]*University of Maryland, College Park, Maryland, 20742, USA*
[3]*University of Edinburgh, Edinburgh, EH9 3JZ United Kingdom*
[4]*University of Notre Dame, Notre Dame, Indiana 46556, USA*
(Received 15 April 2007; published 12 July 2007)

The first data on the relative single-particle energies outside the doubly magic ^{100}Sn nucleus were obtained. A prompt 171.7(6) keV γ-ray transition was correlated with protons emitted following the β decay of ^{101}Sn and is interpreted as the transition between the single-neutron $g_{7/2}$ and $d_{5/2}$ orbitals in ^{101}Sn. This observation provides a stringent test of current nuclear structure models. The measured $\nu g_{7/2}$-$\nu d_{5/2}$ energy splitting is compared with values calculated using mean-field nuclear potentials and is used to calculate low-energy excited states in light Sn isotopes in the framework of the shell model. The correlation technique used in this work offers possibilities for future, more extensive spectroscopy near ^{100}Sn.

It is remarkable that the structure of nuclei, which are assemblies of strongly interacting protons and neutrons, can be approximated so well by nucleons moving independently in an average central potential created by all of them. The symmetries of the potential lead to energy degeneracies, and the available levels are clustered in groups analogous to electron shells in atoms. Nuclei and atoms with filled shells are bound more tightly than their neighbors. Nucleon numbers corresponding to closed shells are called magic. The nuclear magic numbers 2, 8, 20, 28, 50, 82, 126 differ from their atomic counterparts because of the form of their central potentials and the presence of the nuclear spin-orbit interaction, which is strong enough to rearrange the shell gaps. In contrast to atoms, nuclei are two-fermion systems, which results in separate proton and neutron shell structure. Doubly magic nuclei are the cornerstones of the nuclear landscape. The single-particle energies, i.e., eigenvalues of a nucleon in the potential of the core, provide stringent tests of nuclear models. Together with residual interactions between valence nucleons, the single-particle energies are key ingredients in the understanding of multinucleon states in the vicinity of doubly magic nuclei.

The properties of stable doubly magic nuclei, such as ^{16}O, ^{40}Ca, and ^{208}Pb, are quite well known. One of the challenges of contemporary nuclear physics is to explore the extent to which current models can describe nuclei situated far from the line of stability and to develop reliable extrapolations of these models to nuclei which cannot be readily synthesized in a laboratory, but play an important role in astrophysical processes. In this context, data on the exotic doubly magic nuclei ^{48}Ni, ^{78}Ni, ^{100}Sn, and ^{132}Sn are invaluable. In this Letter, we report on the first measurement of the relative position of two single-particle states immediately above the $N = 50$ gap, namely, the $d_{5/2}$ and $g_{7/2}$ neutron states in ^{101}Sn.

The ^{100}Sn region has been studied extensively using a variety of experimental methods. A small number of ^{100}Sn nuclei were detected using fragmentation reactions [1,2], and the ^{100}Sn β-decay half-life of ≈ 1 s was measured. Nuclei around ^{100}Sn can also be produced using heavy-ion induced fusion-evaporation reactions, an approach which can be combined with γ-ray spectroscopic measurements, but the cross sections are very small and experiments are hampered by the presence of a large background. Despite this, a ^{101}Sn β-decay half-life of 3(1) s was obtained and a β-delayed proton spectrum was measured for ^{101}Sn in Ref. [3], and in a recent experiment a more precise half-life of 1.9(3) s was reported [4]. The proton spectrum measured in Refs. [3,4] extends from 1 to 5 MeV with a pronounced maximum around 3 MeV. The production cross section for ^{103}Sn is much larger than for ^{101}Sn, so its β decay properties, including the β-delayed proton branch, have been measured with considerable precision [5]. None of the single-particle or single-hole states relative to ^{100}Sn are known. On the other hand, excited states in ^{103}Sn have been observed using in-beam spectroscopic methods [6]. Also, the first excited state in ^{103}Sn was confirmed by observation of the ^{107}Te α-decay fine structure [7]. In ^{102}Sn, a 6^+ isomer was found [8], and conversion electrons deexciting the isomer were measured in a subsequent experiment [9].

In the present work, prompt γ rays emitted in the production of ^{101}Sn have been identified through correlations with β-delayed protons following the decay of ^{101}Sn using the recoil-decay tagging (RDT) method [10]. The RDT method was used, for example, in first in-beam studies of transfermium nuclei [11,12]. A 192 MeV ^{58}Ni beam from the Argonne Tandem Linac Accelerator system impinged on ≈ 0.8 mg/cm^2 thick isotopically enriched ^{46}Ti targets, mounted on a rotating wheel, to produce ^{101}Sn nuclei after evaporation of 3 neutrons from the

[104]Sn compound nucleus. The targets were irradiated for about 5.5 days at an average beam intensity of 20 pnA. Prompt γ rays were detected in the Gammasphere array of 99 Compton suppressed high purity Ge detectors [13] surrounding the target. Reaction products recoiling from the target (recoils) were separated from the unreacted beam and dispersed according to their mass-to-charge state ratio in the fragment mass analyzer (FMA) [14]. The recoil's position at the FMA focal plane was measured in a parallel grid avalanche counter (PGAC) followed by an ionization chamber (IC) used for energy loss measurement. Recoils with mass number $A = 101$ and charge states 23^+ and 24^+ were accepted by mass slits. After passing through the PGAC-IC combination, the recoiling nuclei were implanted into a 140 μm-thick double-sided silicon strip detector (DSSD). The front and the back sides of the DSSD were divided into 80, 400 μm-wide horizontal and vertical strips forming 6400 pixels. The decays of the implanted nuclei were also observed in the DSSD (anticoincidence with PGAC and IC was required in this case) and in Si detectors surrounding the DSSD: a 300 μm-thick, large area Si detector (LASD) positioned behind the DSSD and a box consisting of four 300 μm-thick single-sided Si strip detectors (SSSD) placed in front of the DSSD. Using spatial and temporal relations in the DSSD, implants were correlated with decays. Characteristic properties of the decays were used to associate prompt γ rays with specific nuclei.

The decay spectrum in the DSSD was dominated by recoils and scattered beam particles that were not always vetoed by the PGAC and the IC. The energy spectrum of decays observed within 5 s of the implantation in coincidence with β particles is presented in the top panel of Fig. 1. A broad energy distribution can be seen with a maximum at about 3 MeV, similar to that assigned to [101]Sn β-delayed protons in Refs. [3,4]. In order to select γ rays associated with [101]Sn, the following decay criteria were considered for tagging. First, the energy deposited in the DSSD had to be between 1.0 and 5.0 MeV and a coincidence with a β particle in the LASD or in one of the SSSDs was required. If the energy deposited in the DSSD was shared between two neighboring front or back strips, the coincidence requirement with the Si detectors was not checked. Second, the decay time had to be shorter than 5 s. The low-energy portion of the γ-ray spectrum tagged by the decay events described above is given in the top panel of Fig. 2. For comparison, γ rays randomly correlated with β particles associated with long-lived activities are included in the middle panel. Indeed, this spectrum is very similar to the ungated singles γ-ray spectrum provided in the bottom panel of Fig. 2. The singles γ-ray spectrum is dominated by γ rays associated with [101]Ag, which was produced after evaporation of 3 protons. Traces of the strongest γ-ray lines from the singles spectrum, such as the 248 keV [101]Ag line, can also be found in the γ-ray spectrum tagged by [101]Sn events. However, a γ-ray line with an energy of 171.7(6) keV composed of 11 counts is

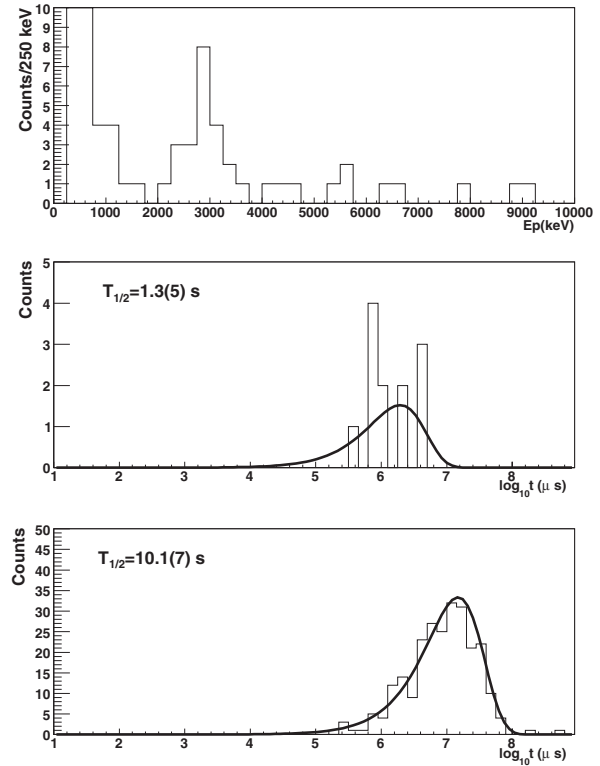
FIG. 1. Top: Spectrum of decays which followed an implant within 5 s and were registered in coincidence with β particles (events below 1 MeV correspond to β particles). Center: Time distribution of protons associated with 172-keV γ rays. Bottom: Time distribution of randomly correlated decay events. The solid lines represent fitted radioactive decay curves corresponding to the half-lives shown.

not present in the random spectrum nor in the singles spectrum. The distribution of decay times for protons gated by 172-keV γ rays is given in the center panel of Fig. 1. It is compared with the time distribution of randomly correlated decays presented in the bottom panel. The 172-keV events are on average about 8 times faster than randomly correlated decays. The radioactive decay curve fits, which can also be found in Fig. 1, resulted in a half-life of 1.3(5) s for the protons associated with the 172-keV γ rays, in agreement with the [101]Sn half-life reported previously [3,4]. Consequently, we assign the 172-keV line to [101]Sn. No other γ-ray transition could be assigned to [101]Sn. In [103]Sn and [105]Sn, there is a ≈1 MeV gap between the pair of low-energy states and the next excitations. This gap is expected to be significantly larger in [101]Sn. The $7/2^+$ level in [103]Sn is fed by two parallel high-energy γ-ray transitions. Detecting equivalent transitions in [101]Sn was below the sensitivity limit of the present measurement.

Light odd-A Sn isotopes exhibit two low-energy levels with spins $7/2^+$ and $5/2^+$. In [103]Sn, the 168-keV transition between them was the strongest prompt γ-ray line observed [6]. These two levels have been associated with a pair of single-neutron orbitals, $d_{5/2}$ and $g_{7/2}$, situated above the $N = 50$ shell gap, as has been extensively dis-
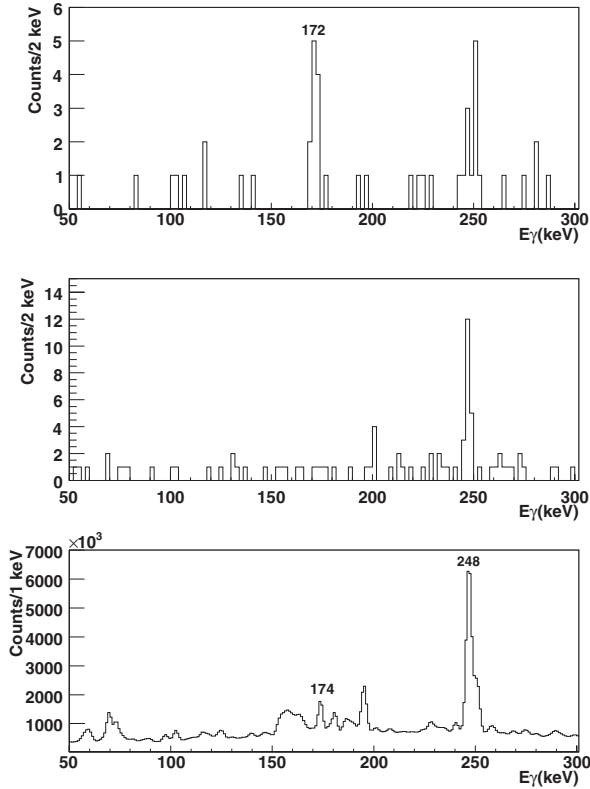
FIG. 2.   Top: Spectrum of γ rays correlated with decay events associated with ^{101}Sn β-delayed protons. Middle: Spectrum of γ rays randomly correlated with β-decay events in the DSSD. Bottom: Total ungated singles γ-ray spectrum. The lines marked with energies correspond to known transitions in ^{101}Ag.
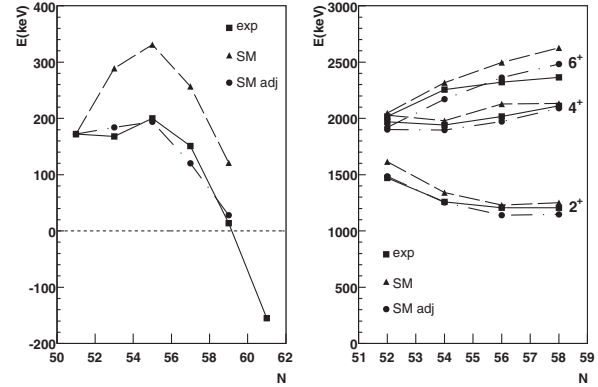

FIG. 3.   Comparison as a function of the neutron number between measured level energies and shell-model calculations for (left) the $7/2^+ - 5/2^+$ energy difference in the light, odd Sn isotopes and (right) the 2^+, 4^+, 6^+ level energies in the even Sn isotopes. The squares connected by solid lines represent measured excitation energies, while triangles (dashed lines) and circles (dot-dashed lines) correspond, respectively, to the shell-model values obtained using the matrix elements of Ref. [22] and with the $(g_{7/2})^2_{0+}$ matrix element reduced by 30%.

cussed in Ref. [15]. The behavior of the $7/2^+ - 5/2^+$ separation energy in odd Sn isotopes can be seen in Fig. 3. The neutron single-particle states associated with the $d_{5/2}$ and $g_{7/2}$ orbitals have also been identified in the $N = 51$ isotones from ^{91}Zr to ^{99}Cd. The $g_{7/2} - d_{5/2}$ energy gap decreases from 2.2 MeV in ^{91}Zr to 441 keV in ^{99}Cd as a result of the strong attraction between the $g_{7/2}$ neutron and the protons gradually filling the $g_{9/2}$ orbital from $Z = 40$ to $Z = 50$. A linear extrapolation to ^{101}Sn places the $g_{7/2}$ state 190 keV above the $d_{5/2}$ ground state, an energy close to the spacing reported here. In view of the above considerations, the 172-keV line is interpreted as a transition between the single-neutron $g_{7/2}$ and $d_{5/2}$ states. It is worth noting that reversed order could lead to a weakly populated nonyrast $d_{5/2}$ state and relatively stronger high-energy transitions feeding the ground state directly, which is not observed here.

The relative single-particle energies can be used to test various forms of the mean-field nuclear potential. In Ref. [16], single-particle energies for the doubly magic nuclei ^{56}Ni, ^{100}Sn, ^{132}Sn, and ^{208}Pb were calculated using the Woods-Saxon potential with the so-called "universal" set of parameters, the folded Yukawa potential, and the self-consistent Hartree-Fock potential obtained with the Skyrme III phenomenological nucleon-nucleon interac-

tion, resulting in $g_{7/2} - d_{5/2}$ energy differences in ^{101}Sn of 1.45, 1.09, and 0.47 MeV, respectively. The self-consistent potential reproduces the measured $g_{7/2} - d_{5/2}$ splitting best. Surprisingly, when a Skyrme interaction was refitted to more recent data across the nuclidic chart, including several single-particle energies, a larger difference of ≈ 1 MeV was obtained [17]. This underlines limitations of current mean-field potentials in predicting single-particle energies. The behavior of single-particle energies in semimagic nuclei can be used to refine these potentials. Recently, the energy separation between the $g_{7/2}$ and $h_{11/2}$ neutron orbitals in the $N = 51$ isotones was reproduced by considering the tensor nature of the nucleon-nucleon interaction [18], and an excitation energy of ≈ 300 keV was predicted for the $\nu g_{7/2}$ state in ^{101}Sn. The self-consistent potential based on the finite-range Gogny nucleon-nucleon interaction [19] and the Skyrme interaction [20] with a tensor component reproduced the trend in the relative positions of the proton $g_{7/2}$ and $h_{11/2}$ orbitals in odd Sb isotopes. The energy of the proton $g_{7/2}$ orbital can be calculated from our measurement by employing the mirror symmetry between ^{101}Sn and ^{101}Sb. If the mass deficits of $-56.780(710)$ and $-59.560(300)$ MeV are used for ^{100}Sn and ^{101}Sn [21], respectively, the binding energies of $-10.07(76)$ and $-9.90(76)$ MeV are obtained for the $\nu g_{7/2}$ and $\nu d_{5/2}$ orbitals. Assuming the Coulomb energy of 14.1 MeV, which is extrapolated from the heavier Sn isotopes, results in a $\pi g_{7/2}$ single-particle energy of 4.4(10) MeV, somewhat larger than a value of ≈ 3 MeV that one gets by extrapolating from heavier Sb isotopes. It would be desirable to establish the role of the tensor effects on the relative neutron and proton $g_{7/2} - d_{5/2}$ energies at ^{100}Sn.
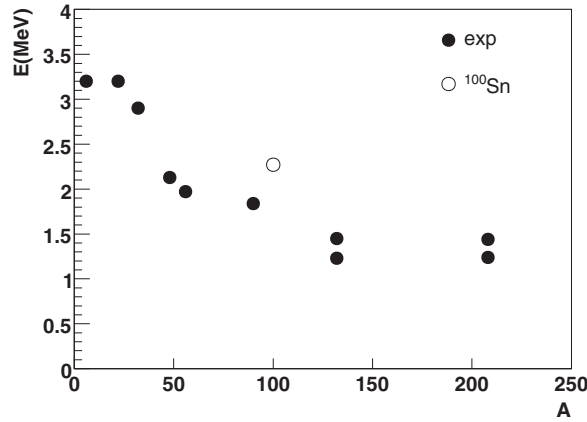
FIG. 4.   The empirical 0^+ residual interaction for doubly magic plus two nucleon nuclei as a function of the mass number. The open circle represents this quantity from the shell-model calculation with the $(g_{7/2})^2_{0+}$ matrix element adjusted, as described in the text. The solid symbols are from Ref. [23], except for the points corresponding to ^{56}Ni and ^{132}Sn, which were obtained from more recent mass measurements.

With the measured energy splitting between the $g_{7/2}$ and $d_{5/2}$ neutron orbitals established, a shell-model calculation of energies of multiparticle configurations in light Sn isotopes was performed. The full $N = 50$–82 shell was available for valence neutrons and the following relative single-particle energies were used in the calculation: $E(d_{5/2}) = 0.0$, $E(g_{7/2}) = 0.172$, $E(s_{1/2}) = 1.55$, $E(d_{3/2}) = 1.65$, and $E(h_{11/2}) = 3.55$ MeV. The effective neutron-neutron interaction, which is the most important ingredient in the calculations after single-particle energies, was taken from Ref. [22], where it was derived from the Bonn C meson-exchange nucleon-nucleon potential in the one-boson-exchange approximation. In the left panel of Fig. 3 the experimental and calculated energies for the two lowest states in the odd Sn isotopes from ^{103}Sn to ^{109}Sn are compared. The shell model predicts the pair of low-lying $7/2^+$ and $5/2^+$ states, with a calculated energy difference that follows the experimental trend closely, but which is about 200 keV too large. Almost perfect agreement with the data can be achieved if the $(g_{7/2})^2_{0+}$ matrix element is reduced from -1.4 to -1.1 MeV. This adjustment preserves the agreement between experiment and theory for the 2^+, 4^+, and 6^+ energies in the even Sn isotopes (see right panel in Fig. 3). Interestingly, reversing the $7/2^+$ and $5/2^+$ states in ^{101}Sn results in a different trend for the $7/2^+ - 5/2^+$ splitting, although the $7/2^+$ level is still located above the ground state in the heavier Sn isotopes. This underlines the ambiguity of extracting the $g_{7/2} - d_{5/2}$ energy difference from ^{103}Sn alone.

In Fig. 4, the calculated energy shift of the 0^+ ground state in ^{102}Sn due to the residual interactions is compared with other experimentally derived 0^+ interactions across the nuclidic chart. Interestingly, the obtained value of 2.27 MeV is slightly larger than the values interpolated

for mass $A \approx 100$ from other doubly magic nuclei. This could be attributed to the strong interaction between the two close lying $g^2_{7/2}$ and $d^2_{5/2}$ 0^+ states in ^{102}Sn.

In summary, an excited state was identified in ^{101}Sn and was interpreted as the $g_{7/2}$ single-neutron state. This is the first observed single-particle state outside the ^{100}Sn core. The deduced neutron $g_{7/2} - d_{5/2}$ energy difference in ^{101}Sn was compared with predictions from various mean-field potentials. The theoretical values have a wide spread and are all substantially larger than the measured energy difference. The variations of the mean field that arise from the tensor force might help reconcile the calculations with the data. The shell-model calculations using the measured relative $g_{7/2} - d_{5/2}$ energy were found to reproduce the trend in the excitation energy of the lowest $7/2^+$ state in light Sn isotopes very well, if the $(g_{7/2})^2_{0+}$ matrix element is reduced by $\approx 30\%$. A higher statistics experiment using the technique used in this work should reveal levels in ^{101}Sn associated either with the breaking of the ^{100}Sn core and/or with the $h_{11/2}$ single-neutron state.

[1] R. Schneider *et al.*, Z. Phys. A **348**, 241 (1994).
[2] M. Lewitowicz *et al.*, Phys. Lett. B **332**, 20 (1994).
[3] Z. Janas *et al.*, GSI Report No. GSI 95-1, 1995, p. 27.
[4] O. Kavatsyuk *et al.*, Eur. Phys. J. A **31**, 319 (2007).
[5] O. Kavatsyuk *et al.*, Eur. Phys. J. A **25**, 211 (2005).
[6] C. Fahlander *et al.*, Phys. Rev. C **63**, 021307(R) (2001).
[7] D. Seweryniak *et al.*, Phys. Rev. C **66**, 051307(R) (2002).
[8] M. Lipoglavsek *et al.*, Z. Phys. A **356**, 239 (1996).
[9] M. Lipoglavsek *et al.*, Phys. Lett. B **440**, 246 (1998).
[10] E. S. Paul *et al.*, Phys. Rev. C **51**, 78 (1995).
[11] P. Reiter *et al.*, Phys. Rev. Lett. **82**, 509 (1999).
[12] M. Leino *et al.*, Eur. Phys. J. A **6**, 63 (1999).
[13] R. V. F. Janssens and F. S. Stephens *et al.*, Nucl. Phys. News **6**, 9 (1996).
[14] C. N. Davids *et al.*, Nucl. Instrum. Methods Phys. Res., Sect. B **70**, 358 (1992).
[15] J. J. Ressler *et al.*, Phys. Rev. C **65**, 044330 (2002).
[16] G. A. Leander *et al.*, Phys. Rev. C **30**, 416 (1984).
[17] B. A. Brown, Phys. Rev. C **58**, 220 (1998).
[18] T. Otsuka *et al.*, Phys. Rev. Lett. **95**, 232502 (2005).
[19] T. Otsuka, T. Matsuo, and D. Abe, Phys. Rev. Lett. **97**, 162501 (2006).
[20] B. A. Brown *et al.*, Phys. Rev. C **74**, 061303(R) (2006).
[21] A. H. Wapstra, G. Audi, and C. Thibault, Nucl. Phys. **A729**, 129 (2003).
[22] M. Hjorth-Jensen, T. T. S. Kuo, and E. Osnes, Phys. Rep. **261**, 125 (1995).
[23] J. P. Schiffer and W. W. True, Rev. Mod. Phys. **48**, 191 (1976).